Lower reflectivity and higher minority carrier lifetime of hand-tailored porous silicon*

Zhang Nansheng(张楠生)†, Ma Zhongquan(马忠权), Zhou Chengyue(周呈悦), and He Bo(何波)

(SHU-SolarE R&D Laboratory, Department of Physics, Shanghai University, Shanghai 200444, China)

Abstract: Solar cell grade crystalline silicon with very low reflectivity has been obtained by electrochemically selective erosion. The porous silicon (PS) structure with a mixture of nano- and micro-crystals shows good antireflection properties on the surface layer, which has potential for application in commercial silicon photovoltaic devices after optimization. The morphology and reflectivity of the PS layers are easily modulated by controlling the electrochemical formation conditions (i.e., the current density and the anodization time). It has been shown that much a lower reflectivity of approximately 1.42% in the range 380–1100 nm is realized by using optimized conditions. In addition, the minority carrier lifetime of the PS after removing the phosphorus silicon layer is measured to be ~3.19 μs. These values are very close to the reflectivity and the minority carrier lifetime of Si_3N_4 as a passivation layer on a bulk silicon-based solar cell (0.33% and 3.03 μs, respectively).

Key words: porous silicon; reflectivity; minority carrier lifetime
DOI: 10.1088/1674-4926/30/7/072004 **EEACC:** 2520

1. Introduction

Good optical antireflection layers (ARL) and textured morphologies realized on bulk silicon-based solar cells are significant for high efficiency solar cells. In previous work, many kinds of ARL materials, such as SiO_2, TiO_2, Si_3N_4, SiO_xN_y, Ta_2O_5, and tri-layer antireflection coatings (SiO_2/SiO_2–TiO_2/TiO_2)[1–6] have been widely developed for the simple diode. Recently, a few of works looked at porous silicon layers (PSL) for the use in ARL[7–9]. It was reported by Strehlke *et al.*[7] that the reflectivity of porous silicon fabricated by anodic electrochemical etching in an electrolyte was approximately 7.3% higher in the wavelength range of 400–1150 nm. A constant current density of 5 mA/cm^2 was used in a solution of 30% HF with a volume ratio of 3 : 2 (48% HF : EtOH). The PSL can be formed on all kinds of single-crystalline silicon and multi-crystalline silicon. However, the traditional method for the formation of a textured surface on silicon in NaOH or KOH is only available in the ⟨100⟩ normal to the surface. Solar cell processing is subject to rigorous limitation.

In the present work, the PSL was formed by the electrochemical etching. The reflectivity, the minority carrier lifetime and the photon-trap structure of the PSL were investigated and compared with other results. The reflectivity of porous silicon (PS) has been successfully reduced to 1.42% by optimizing the anodic current density and the etching time. Furthermore, it was found that the passivation effect of PS as an antireflection coating layer was very similar to that of Si_3N_4.

2. Experiment

For comparison, the slices of the silicon crystals were divided into six groups (A–F), depending on the different treatments. Group A was passivated with Si_3N_4 by PECVD. Group B was non-treated silicon. Group C was thinned silicon. Group D was thinned silicon, which was subsequently pre-textured. Group E was treated in several steps by thinning, pre-texturing, diffusion for producing the n^+p junction, removal for a phosphorus silicon glass layer, etching for the n^+ edge region, and Si_3N_4 passivation processing. Group F was porous silicon before diffusion.

During sample preparation, a ⟨100⟩ oriented p-type CZ silicon wafer with a resistivity of 1 Ω·cm and a thickness of 220 μm was used. The substrate was ultrasonically etched in NaOH : H_2O (1 : 5, at 80 °C for 1 min) in order to remove the damaged machined layer. An Al back contact grid as the anode was deposited by screen printing, followed by annealing at high temperature in a routine technique used in industrial processes.

The controllable morphology of the PSL was formed through a normal electrochemical technique as follows: the electrolyte was a mixed solution of HF : H_2O : C_2H_5OH (2 : 1 : 1 volume ratio). A platinum rod was used as a cathode. A PS layer was ultrasonically (40 Hz) formed at 40 °C for 40 s under an anodic current density of 5 mA/cm^2 on the n^+ region.

The variation of minority carrier lifetime with fabrication

* Project supported by the National Natural Science Foundation of China (No. 60876045) and the Innovation Foundation of Shanghai Education Committee (No. 08YZ12).

† Corresponding author. Email: ioryzns@shu.edu.cn

Received 28 November 2008, revised manuscript received 27 February 2009

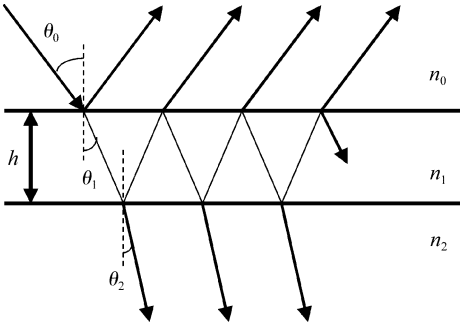

Fig. 1. Reflectivity and refraction of a single film layer.

processing of a solar cell, after the procedures of wafer thinning, PSL formation, phosphorus diffusion, phosphorus silicon glass removal, and silicon edge etching, are addressed. Since it is hard to remove Al deposited on silicon by screen printing in HF and due to Al contamination in the diffusion chamber, in this work, PSL was formed by using the Al vaporized on the back of the silicon as an anode and the minority carrier lifetime was measured at room temperature. The PSL was cleaned in HF and HCl before the diffusion. The n^+p junction was produced in our laboratory. A phosphorus silicon glass layer was removed in a mixed solution of HF and H_2O. The n^+ edge region of the sample was etched in mixed gases of CF_4 and O_2.

During the characterization of the microstructures and the properties of the PSL, the reflectivity of those samples (A–F) was measured in our laboratory by a comprehensive opto-electric analysis system specialized for the internal quantum efficiency (iQE), the external quantum efficiency (eQE), and photoluminescence (PL). It consists of a 250 W halogen-tungsten lamp, a Jobin Yvon spectroscopy, a 7-STAR 7ISW303 monochromator, a DR004-2.0 integrating sphere, a Stanford SR540 light chopper, and an SR830 lock-in amplifier.

The minority carrier lifetime of the PSL after removing the phosphorus silicon layer was measured and compared with that of Si_3N_4 by the microwave reflectance photoconductivity decay with a WT-1000 wafer tester[10]. The morphology of the photon-trap structure on PSL was observed by a scanning electron microscopy (SEM).

3. Results and discussion

3.1. Reflectivity

The ARC effect based on internal multiple reflections between reflected waves at the air/ARC layer and the ARC layer/substrate interfaces is shown in Fig. 1. The reflectivity R is given as a function of the refractive index n_0 of air, the refractive index n_1 of the PSL, and the refractive index n_2 of the substrate. It is given by

$$R = \frac{(n_0 - n_2)^2 \cos^2\frac{\phi}{2} + \left(\frac{n_0 n_2}{n_1} - n_1\right)^2 \sin^2\frac{\phi}{2}}{(n_0 + n_2)^2 \cos^2\frac{\phi}{2} + \left(\frac{n_0 n_2}{n_1} + n_1\right)^2 \sin^2\frac{\phi}{2}} \quad (1)$$

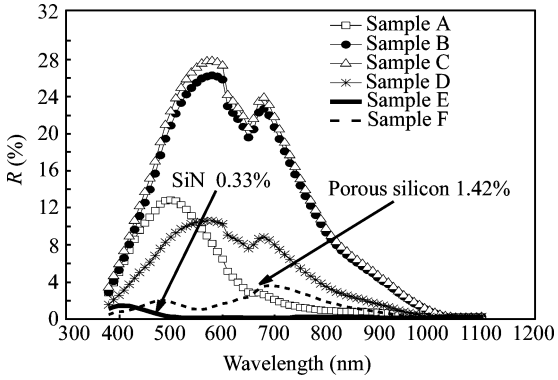

Fig. 2. Reflectivity of samples A, B, C, D, E, and F is shown for comparison.

$$\phi = \frac{4\pi}{\lambda} n_1 h \cos\theta_1 \quad (2)$$

When $n_1 h = (2m + 1)\lambda/4$, $m = 1, 2, 3\ldots$, $\cos^2(\phi/2) = 0$, and $\sin^2(\phi/2) = 1$, then

$$R = \left(\frac{n_0 n_2 - n_1^2}{n_0 n_2 + n_1^2}\right)^2. \quad (3)$$

On the other hand, when $n_1 = \sqrt{n_0 n_2}$, then $R_{\min} = 0$. The effective reflectivity R_{total} was calculated by normalizing the reflectivity R to the photon flux $J(\lambda)$ of the solar spectrum, under AM1.5 standard conditions[7] :

$$R_{\text{total}} = \frac{\int R(\lambda) J(\lambda)\,\mathrm{d}\lambda}{\int J(\lambda)\,\mathrm{d}\lambda}. \quad (4)$$

Furthermore, the refractive index n_1 of the PS is also a function of the porosity f_{air} according to the equation as follows[7] :

$$1 - f_{\text{air}} = \frac{\left(1 - n_1^2\right)\left(n_2^2 + 2n_1^2\right)}{3n_1^2\left(1 - n_2^2\right)}. \quad (5)$$

The theoretical short-circuit current of the junctions, I_{SC}, under white light illumination (AM1.5), has been calculated from the measured reflectivity R, by

$$\text{iQE}(\lambda) = \text{eQE}(\lambda) / (1 - R), \quad (6)$$

$$I_{\text{SC}} = q\int \text{eQE}(\lambda) J_0^{\text{AM1.5}}(\lambda)\,\mathrm{d}\lambda, \quad (7)$$

where $J_0^{\text{AM1.5}}$ is the solar photon flux. According to Eqs. (6) and (7)[7, 11], the decrease of the reflectivity can enhance the short circuit current I_{SC}.

The reflection spectra of the different samples are shown in Fig. 2. It can be seen that the effective reflectivity of the PSL is reduced to 1.42% between 380 and 1100 nm. It exceeds the reflectivity of the sample D and is close to the reflectivity of the sample E (0.33%). A minimum of the reflectivity in Fig. 2 is observed, and its intensity, $R_{\min}$, as well as the position at 550 nm, where the energy content of the solar spectrum peaks, is strongly dependent on the current density used to control the thickness and the porosity of PSLs. All spectra modulated by interference fringes with a long period lead to a broadened minimum. Reflectance spectra are used as criteria to determine the conditions under which the appropriate thickness of the

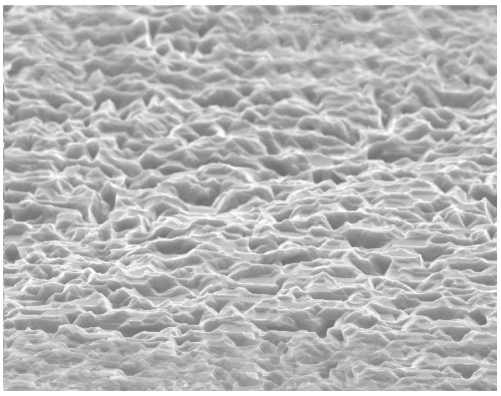

Fig. 3. SEM image of the PSL surface.

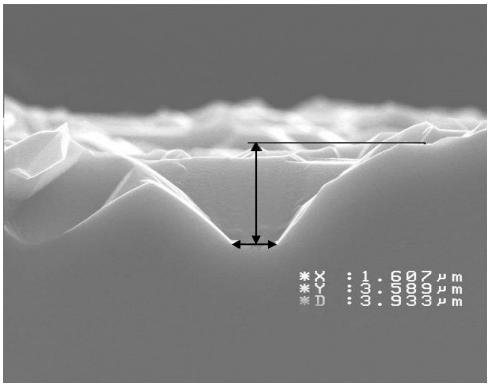

Fig. 4. Cross-section of the SEM image of a pore in the PSL.

PSL is obtained. Comparison of the reflection spectra indicates that the minimum integrated reflectance values in the wavelength range can fulfill a certain application.

3.2. Minority carrier lifetime

The theoretical open-circuit voltage of the junction, V_{OC}, under white light illumination (AM1.5), has been calculated from the measured minority carrier lifetime, by using the following equations in an ideal diode[11]:

$$qV_{OC} = kT \ln\left(\frac{I_{SC}}{I_0} + 1\right), \tag{8}$$

$$I_{SC} = q\overline{G}A\left(\sqrt{D_n\tau_n} + \sqrt{D_p\tau_p}\right), \tag{9}$$

$$I_0 = Aqn^2\left(\frac{\sqrt{D_p}}{N_D\sqrt{\tau_p}} + \frac{\sqrt{D_n}}{N_A\sqrt{\tau_n}}\right), \tag{10}$$

where A is the area of junctions, $\overline{G}$ is the average production rate of the non-equilibrium carrier in the diffusion length (L_n + L_p) of the junction, I_0 is the reverse saturated current, n is the same ideality factor, D_p and D_n are the hole and electron diffusion coefficients, and τ_p and τ_n are the lifetimes of holes and electrons, respectively. The increase of the minority carrier lifetime can lead to an increase of V_{oc} according to Eqs. (8)–(10).

The minority carrier lifetime of the PS after removing the phosphorus silicon layer is obviously longer (3.19 μs) than that of sample F (3.03 μs). This result suggests that the PS with a higher minority carrier lifetime could potentially act as a substitute for Si_3N_4 material in passivation layers on silicon-based solar cells.

Actually, the total value of the minority carrier lifetime τ_{total} depends on that in the bulk material τ_{bulk}, the characteristic time necessary to allow carrier diffusion to the surface from the middle of the wafer τ_{diff}, and the characteristic time of surface recombination τ_{surf}. It is given as:

$$\frac{1}{\tau_{total}} = \frac{1}{\tau_{bulk}} + \frac{1}{\tau_{diff} + \tau_{surf}}. \tag{11}$$

In the experiment, it is found that removing the phosphorus silicon glass layer can reduce the minority carrier lifetime of silicon from 10 to 3.03 μs when it was thinned, subsequently pre-textured and diffused. The reason for this is that the decrease of τ_{surf} can lead to a decrease of τ_{total} according to Eq. (11).

3.3. Profile of the PS surface

The surface morphology and features of the PSL are shown in Fig. 3. The lateral distribution of the surface roughness is typical for the PSL among the electrochemical etched samples. The shape and the size of a pore are shown in Fig. 4. Three dimensions of the typical pore were illustrated as X: 1.607, Y: 3.589, and D: 3.933 μm, respectively. The depth of the pore are in this figure is about 3.60 μm, which is less than that of a n^+p junction of a bulk silicon-based solar cell with a typical depth value of approximately 0.45 μm. Therefore, the anodization regimes (the current density and etching time) must be selected so as to prevent the thickness of the PS layer from exceeding the depth of a n^+p junction, if the PS is formed before the diffusion. In an optimized process, the miniaturized PSL with a lower reflectivity can be obtained by increasing the concentration of HF in the electrolyte and choosing a polished silicon with a lower resistivity of about 0.01 Ω·cm.

4. Conclusion

A very low reflectivity from a PS surface has been obtained by the electrochemical etching treatment of bulk silicon in any orientation. The current density and the etching time are essential parameters in the processing. The condition in our research is a combination of the electrolyte with a mixed solution of HF : H_2O : C_2H_5OH (2 : 1 : 1 volume ratio), a platinum rod used as the cathode, and the PSL being ultrasonically (40 Hz) formed at 40 °C for 40 s under an anodic current density of 5 mA/cm^2 on the n^+ region.

In addition, the improvement of the minority carrier lifetime for the PSL lies obviously in the electrochemical processing, which implies a possible application in the photovoltaic industry as a convenient and inexpensive technique.

Acknowledgements

Part of the process was completed by Solar Enertech

(Shanghai) Co. Ltd. We appreciate Dr. Tang Yinghui, Mr. Yu Zhengshan, Mr. Ying Yanting, and Mr. Lu Peng for their support on the thermal diffusion, the PECVD, and the edge etching of the cells.

References

[1] Song L, Xu H, Chen Q, et al. Low reflective SiO_2 coatings prepared by the sol-gel process. Glass & Enamel, 1994, 23(3): 8

[2] Wang H, Ba D, Shen H, et al. Fabrication and characterization of TiO_2 antireflection thin film deposited on the solar cell. Proceedings of the 8th Vacuum Metallurgy and Surface Engineering Conference, 2007

[3] Liu Z, Zhang Z, Li H, et al. Comparing research on TiO_2 antireflection coating (ARC) and SiN ARC of crystalline Si solar cell. Journal of Kunming Teachers College, 2003, 25(4): 75

[4] Lipinski M, Kaminski A, Lelievre J F, et al. Investigation of graded index SiO_xN_y antireflection coating for silicon solar cell manufacturing. Phys Status Solidi C, 2007, 4(4): 1566

[5] Wei Jinyun, Liu Tao. Ta_2O_5 antireflection thin films for PV application with reactive R–F sputtering technique in low vacuum. Acta Energiae Solaris Sinica, 1998, 19(3): 109

[6] Lien S, Wuu D, Yeh W, et al. Tri-layer antireflection coatings (SiO_2/SiO_2–TiO_2/TiO_2) for silicon solar cells using a sol–gel technique. Solar Energy Materials & Solar Cells, 2006, 90: 2710

[7] Strehlke S, Bastide S, LeHvy-CleHment C. Optimization of porous silicon reflectance for silicon photovoltaic cells. Solar Energy Materials & Solar Cells, 1999, 58: 399

[8] Vitanov P, Delibasheva M, Goranova E, et al. The influence of porous silicon coating on silicon solar cells with different emitter thicknesses. Solar Energy Materials & Solar Cells, 2000, 61: 213

[9] Adamian Z N, Hakhoyan A P, Aroutiounian V M, et al. Investigations of solar cells with porous silicon as antireflection layer. Solar Energy Materials & Solar Cells, 2000, 64: 347

[10] Wang Zhengqiu, Gong Haimei, Li Yanjin, et al. Study of minority carrier lifetime in semiconductors by contactless measurement method: microwave reflectance technique. Journal of Infrared and Millimeter Waves, 1996, 15(1): 78

[11] Metzger W K. How lifetime fluctuations, grain-boundary recombination, and junctions affect lifetime measurements and their correlation to silicon solar cell performance. Solar Energy Materials & Solar Cells, 2008, 92: 1123